
Article:
Llewellyn, R.D.O., Bentley, M.A. orcid.org/0000-0001-8401-3455, Wadsworth, R. orcid.org/0000-0002-4187-3102 et al. (23 more authors) (2020) Spectroscopy of proton-rich 79Zr:Mirror energy differences in the highly-deformed fpg shell. Physics Letters B. 135873. ISSN: 0370-2693

https://doi.org/10.1016/j.physletb.2020.135873

Physics Letters B 811 (2020) 135873

Contents lists available at ScienceDirect

Physics Letters B

www.elsevier.com/locate/physletb

Spectroscopy of proton-rich ^{79}Zr: Mirror energy differences in the highly-deformed *fpg* shell

R.D.O. Llewellyn [a,*], M.A. Bentley [a,*], R. Wadsworth [a], J. Dobaczewski [a,b], W. Satuła [b], H. Iwasaki [c,d], G. de Angelis [e], J. Ash [c,d], D. Bazin [c,d], P.C. Bender [c,1], B. Cederwall [f], B.P. Crider [c,2], M. Doncel [g], R. Elder [c,d], B. Elman [c,d], A. Gade [c,d], M. Grinder [c,d], T. Haylett [a], D.G. Jenkins [a], I.Y. Lee [h], B. Longfellow [c,d], E. Lunderberg [c,d], T. Mijatović [c,3], S.A. Milne [a], D. Rhodes [c,d], D. Weisshaar [c]

[a] Department of Physics, University of York, Heslington, York YO10 5DD, United Kingdom
[b] Institute of Theoretical Physics, Faculty of Physics, University of Warsaw, ul. Pasteura 5, PL-02-093 Warsaw, Poland
[c] National Superconducting Cyclotron Laboratory, Michigan State University, East Lansing, MI 48824, USA
[d] Department of Physics and Astronomy, Michigan State University, East Lansing, MI 48824, USA
[e] Legnaro National Laboratory, 35020 Legnaro, Italy
[f] KTH Department of Physics, S-10691 Stockholm, Sweden
[g] Department of Physics, University of Liverpool, Liverpool L69 3BX, United Kingdom
[h] Nuclear Science Division, Lawrence Berkeley National Laboratory, Berkeley, CA 94720, USA

ARTICLE INFO

Article history:
Received 3 July 2020
Received in revised form 5 October 2020
Accepted 14 October 2020
Available online 19 October 2020
Editor: D.F. Geesaman

ABSTRACT

Energy differences between isobaric analogue states have been extracted for the $A = 79$, ^{79}Zr/^{79}Y mirror pair following their population via nucleon-knockout reactions from intermediate-energy rare-isotope beams. These are the heaviest nuclei where such measurements have been made to date. The deduced mirror energy differences (MED) are compared with predictions from a new density-functional based approach, incorporating isospin-breaking effects of both Coulomb and nuclear charge-symmetry breaking and configuration mixing.

1. Introduction

The approximately charge-symmetric and charge-independent nature of the nuclear force [1] yields very strong symmetries between particular (analogue) states in nuclei with the same mass number, A. This led to the powerful concept of the isospin quantum number t, which characterises neutrons and protons as separate states of a nucleon with isospin projections of $t_z = +\frac{1}{2}$ and $-\frac{1}{2}$, respectively [2]. Likewise, the total isospin projection T_z of a nucleus is defined as $T_z = (N - Z)/2$. States of the same isospin among a set of nuclei with the same A, but different T_z (Isobaric Analogue States, IAS) would, in the limit of perfect isospin symmetry, be degenerate. Whilst this is never precisely the case, a strong degree of symmetry always remains in mirror nuclei since the effects that break the symmetry are sufficiently weak that they may be considered a perturbation, and do not significantly alter the symmetry of the underlying wave functions.

Observed discrepancies between the excitation energies of isobaric multiplets can be attributed to the presence of isospin-violating interactions originating from Coulomb and magnetic effects, as well as isospin-nonconserving (INC) components of the nucleon-nucleon interaction. In mirror nuclei, such energy differences, termed Mirror Energy Differences (MED), are of isovector origin and are defined as:

$$\mathrm{MED}_J = E^*_{J,T,-T_z} - E^*_{J,T,T_z}, \tag{1}$$

where E^*_{J,T,T_z} is the excitation energy of a given state with spin J and isospin T of a nucleus with $\pm T_z$. Theoretical modelling of MED has conventionally taken place within a shell-model framework – see e.g. refs. [3–7] and references therein. Here the electromagnetic effects, of multipole and monopole nature, are included through

* Corresponding authors.
E-mail addresses: ryan.llewellyn@york.ac.uk (R.D.O. Llewellyn), michael.bentley@york.ac.uk (M.A. Bentley).
[1] Present address: Department of Physics, University of Massachusetts Lowell, Lowell, Massachusetts 01854, USA.
[2] Present address: Department of Physics and Astronomy, Mississippi State University, Mississippi State, Mississippi 39762, USA.
[3] Present address: Ruđer Bošković Institute, HR-10·001 Zagreb, Croatia.

https://doi.org/10.1016/j.physletb.2020.135873

modifications to the effective interactions and single-particle levels in the shell-model framework. This has been, on the whole, very successful. It was also found that in order to obtain good agreement with the data, large additional two-body isospin non-conserving matrix elements needed to be included, which have a contribution to the MED of the same order as that of the Coulomb effect [4,6].

Modern developments in experimental techniques have opened a gateway to the study of neutron-deficient $N \approx Z$ nuclei in the $A = 60 - 80$ region, enabling MED studies within the upper fp shells (e.g. [8–11]). Similar shell-model approaches have been applied and, again, for mirror nuclei, large additional isovector INC terms were required [10,12]. The need for inclusion of large INC terms points to physics not contained within the shell-model approach. A fundamental understanding of such isospin-symmetry breaking phenomena, and how they might be included in nuclear models, is important – for example in predicting the location of drip lines, where the inclusion of INC effects in shell-model calculations has been found necessary to replicate experimental observations [13].

The current work presents results for the heaviest mirror pair for which MED have been measured to date, and the first in the well-deformed $A \sim 80$ region of nuclei – the $A = 79$, $T_z = \pm\frac{1}{2}$ ^{79}Zr/^{79}Y mirror pair. This has been made possible through the observation of excited states for the proton-rich $Z = 40$ system ^{79}Zr. A reliable shell-model interpretation of nuclei in this region (the centre of the fpg shell near $A = 80$) is not currently feasible due to the size of the valence space required, since it is known that in this highly-deformed region the inclusion of orbitals originating from above the ^{100}Sn core are required [14]. In the work presented here, we interpret the results through a new theoretical approach to MED, rooted in density-functional theory, using a development of the no-core configuration-interaction (NCCI) model [15] designed to allow for the study of isospin-breaking effects among excited states.

2. Experimental procedure

The experiment was performed at the National Superconducting Cyclotron Laboratory (NSCL) at Michigan State University. Following initial acceleration of a ^{92}Mo beam by the K500 and K1200 cyclotrons [16] to 140 MeV/u, the beam was fragmented by a thick ^{9}Be target at the entrance to the A1900 separator [17]. The reaction products were separated via the A1900 with a momentum acceptance of 0.5% producing a cocktail beam consisting of primarily 0.3% ^{81}Zr, 5.0% ^{80}Y, 22.8% ^{79}Sr, 48.2% ^{78}Rb and 21.6% ^{77}Kr. These products impinged upon a 188 mg/cm^2 ^{9}Be reaction target located at the S800 target position. De-excitation γ rays from the nuclei populated at the reaction target position were detected with the Gamma-Ray Energy Tracking In-beam Nuclear Array (GRETINA) [18,19] in a ten module configuration, with four modules centred at 57° and six centred at 90°, covering laboratory angles of 37° to 116°. Reaction products were separated by the S800 magnetic spectrograph [20] and identified via time of flight and energy-loss information acquired with a series of scintillators and an ionisation chamber located within the spectrograph. ^{79}Zr ($T_z = -\frac{1}{2}$) was populated via a two-neutron knockout reaction from the ^{81}Zr ($T_z = +\frac{1}{2}$) secondary beam, a reaction mechanism previously utilised to examine mirror states in the $A = 50$ region [5]. Likewise, ^{79}Y ($T_z = +\frac{1}{2}$) was produced via one-neutron knockout from the ^{80}Y ($T_z = +1$) secondary beam. Further detail about the particle-identification for this experiment, including sample particle-identification plots, can be found in Ref. [21].

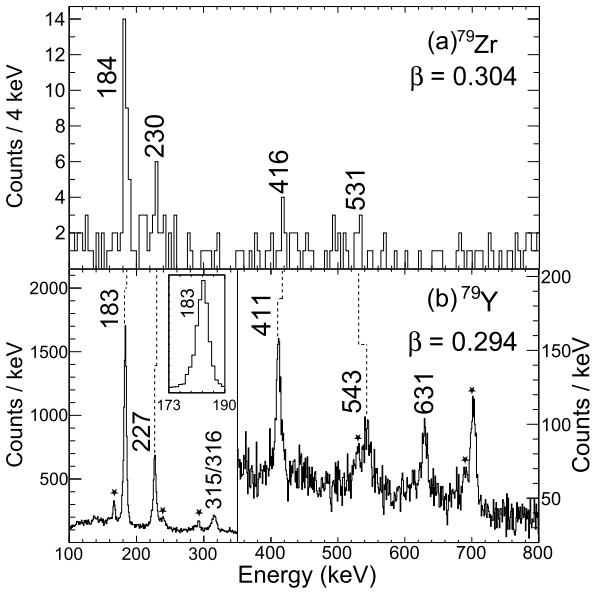

Fig. 1. The Doppler-corrected spectra for (a) ^{79}Zr and (b) ^{79}Y corrected with the indicated β values. β in (a) is optimised for faster decays whilst in (b) a slower β is chosen to show the lineshape of the 183-keV peak (see text for details). The inset of (b) displays an expanded view of the 183-keV, $(\frac{7}{2}^+) \rightarrow (\frac{5}{2}^+)$ decay where a low-energy lineshape is visible. The dashed lines indicate the analogue transitions of the $A = 79$ mirror pair. New, unplaced, decays in ^{79}Y are indicated with stars.

3. Results

The trajectories and momentum distributions of the recoiling reaction products were measured in the S800 spectrograph, and this information was combined with the measured first γ-ray interaction point in the GRETINA array to enable precise event-by-event γ-ray Doppler corrections. The resulting spectrum measured in coincidence with ^{79}Y recoils is shown in Fig. 1(b). The transitions labelled in Fig. 1(b), have previously been assigned to the ground-state band of ^{79}Y, where spins and parities have only been tentatively assigned [22]. The structure was interpreted as a rotational sequence built upon a presumed $[422]\frac{5}{2}^+$ Nilsson configuration. The sequence of γ rays observed in ^{79}Y in this work is shown in the partial level scheme on the right of Fig. 2. Determination of the optimum recoil velocity for the Doppler-correction analysis for a particular spectral line is crucial for this analysis, and is achieved in this work by varying the recoil velocity ($\beta = \frac{v}{c}$) until any dependence of the Doppler-corrected γ-ray energy on the GRETINA polar angle (θ) is eliminated. This technique is demonstrated in Fig. 3 for the three lowest-energy transitions in ^{79}Y. For the known 184-keV $(\frac{7}{2}^+) \rightarrow (\frac{5}{2}^+)$ transition [22] in ^{79}Y, this yields an optimum after-target recoil velocity ($\beta = \frac{v}{c}$) of 0.294 [see Fig. 3(a)] and this is the value used for Fig. 1(b). The 227 and 411-keV γ rays in ^{79}Y were found to be best optimised at a slightly higher value of $\beta = 0.296$, whilst the remaining observed transitions in ^{79}Y required $\beta = 0.304$ to optimise the spectrum [Fig. 3(b)]. With the exception of the 184 keV-transition (see below) all energies are found to agree well with those of Ref. [22] (see Table 1). The transit time from the front to the back of the target of the recoiling nuclei travelling with $\beta = 0.3$ is of the order of 10 ps. Hence decays occurring on this time scale will occur at different average points within the target, resulting in different energy loss of the recoil in the target and hence marginally different β values.

Evidence of a small low-energy tail on the 183(1)-keV transition can be seen in the inset of Fig. 1(b), suggesting a lifetime of several tens of picoseconds. Similar spectroscopic effects have been observed previously for decays from low-lying states in well de-

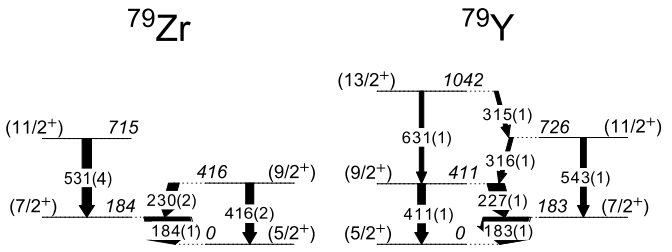

Fig. 2. The tentative γ-ray scheme of ^{79}Zr compared with that of ^{79}Y. Note the slight discrepancy between the sum of the γ-ray energies between the $(\frac{9}{2}^+) \rightarrow (\frac{7}{2}^+) \rightarrow (\frac{5}{2}^+)$ decays and the direct $(\frac{9}{2}^+) \rightarrow (\frac{5}{2}^+)$ decay most likely arises from lifetime effects (see text for details) as well as uncertainties on the individual γ-ray energies. The numbers in brackets after the γ-ray energies represent the assigned errors on these decays from the present work.

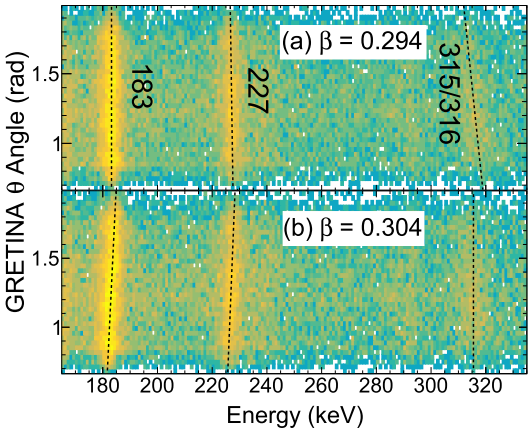

Fig. 3. Doppler-corrected γ-ray spectra for ^{79}Y against the detected polar angle of GRETINA, corrected with the indicated recoil velocities. It is clear that a slower recoil velocity is required to correct the 183-keV transition, panel (a), compared to that needed to optimise transitions such as the 315/316-keV decays, which predominantly occur whilst the recoil is within the target, panel (b). The latter transitions are expected to decay from shorter lived (few ps) states. The dashed black lines are to guide the eye.

formed nuclei from this mass region [21,23]. The small, ∼1-keV discrepancy between the previously measured value of 184.0(5) keV [22] and the 183(1) keV determined from the present work is likely to be a consequence of this lifetime effect since a γ decay taking place significantly downstream of the target will result in a small downward shift in the peak centroid energy.

In addition to the previously known transitions in ^{79}Y some new, weak γ rays are observed in the present work – see Fig. 1(b). These are believed to be either members of a new, previously unobserved, rotational structure, or decays connecting this structure to other band structures. The limited $\gamma-\gamma$ statistics in the present work prevented a more detailed analysis of these data. The errors given with the γ-ray energies incorporate uncertainties associated with recoil velocity, reaction target position as well as the effects of different degrees of spectral compression that have been used to extract the transition energies.

Fig. 1(a) shows tentative evidence for four new γ rays measured in coincidence with $T_z = -\frac{1}{2}$ ^{79}Zr recoils. For the degree of compression used for the ^{79}Zr spectrum in Fig. 1(a), γ-ray peaks would be expected to have a width of 2-3 channels, since the measured FWHM of the 411-keV peak of ^{79}Y shown in Fig. 1(b) is ∼9 keV. Although the statistics are very low in Fig. 1(a), the strong similarities observed between the tentative peak positions in this spectrum and those shown in Fig. 1(b) for ^{79}Y, gives confidence to the identification of these transitions. Mirror symmetry arguments are therefore applied to produce the tentative level scheme shown on the left of Fig. 2. Although the reaction processes are somewhat different for the two mirror nuclei (see below), it appears that the analogue ground-state structures are populated in the two reactions.

By employing the same Doppler-correction procedure to that used for ^{79}Y, an optimum beam velocity of $\beta = 0.298$ was found for the 184-keV transition in ^{79}Zr, although the statistics were too weak to perform a similar procedure to that used in ^{79}Y for the higher energy γ rays. Optimisation of the spectral quality by eye yielded a β of 0.304 for the higher energy transitions. The observation that a higher β is required for the higher-energy transitions in the spectrum is consistent with our observations for ^{79}Y. Based on mirror-symmetry arguments, one would expect the 184-keV transition in ^{79}Zr to decay from a state with a similar lifetime to that of its analogue in ^{79}Y, which in turn suggests that the decay may also be expected to occur downstream of the target with a lower recoil velocity, again resulting in a downward shift of the peak centroid energy. This is the likely explanation for the fact that, in both nuclei, the sum of the observed γ-ray energies for the $(\frac{7}{2}^+) \rightarrow (\frac{5}{2}^+)$ and $(\frac{9}{2}^+) \rightarrow (\frac{7}{2}^+)$ decays do not quite add up to the energy of the decay observed for the cross-over $(\frac{9}{2}^+) \rightarrow (\frac{5}{2}^+)$ E2 decay. From this analysis, the measured γ-ray energies and relative intensities for the observed transitions in each nucleus are summarised in Table 1. The branching ratios of decays from the $(\frac{9}{2}^+)$ states are found to be consistent, within errors, across both nuclei.

Both reactions used to generate the spectra in Fig. 1 (^{81}Zr−2n and ^{80}Y−1n, respectively) are direct reactions and it is possible to consolidate the experimental observations by considering the direct population routes to the observed states. Production cross sections are estimated to be 2.9 mb for ^{79}Y and 0.4 mb for ^{79}Zr from their corresponding secondary beams. For the ^{80}Y−1n reaction, the odd-odd fragment beam will likely be in either the tentatively assigned (4^-) ground-state or one of the low-lying isomers tentatively assigned as (1^-) and (2^+). Considering direct removal of a neutron from of any of the $f_{\frac{5}{2}}$, $p_{\frac{3}{2},\frac{1}{2}}$, $g_{\frac{9}{2}}$ orbitals likely to dominate the configurations involved in this region, the maximum-spin positive-parity state that can be directly populated in all reactions is $\frac{13}{2}^+$. This is completely consistent with our experimental observations for ^{79}Y, where no known decays from states above $\frac{13}{2}^+$ are observed. Similarly, positive-parity states in ^{79}Zr can be directly populated from the $(\frac{3}{2}^-)$ ground state of ^{81}Zr by two-neutron removal from a pair of orbitals of opposite parity. Considering the same available fpg orbitals, all the tentative states identified in ^{79}Zr can be populated in all the direct routes allowed by parity and angular-momentum conservation.

Table 1 contains the excitation energies of the tentatively assigned states in ^{79}Zr/^{79}Y. The errors presented with the γ-ray energies incorporate uncertainties associated with the recoil velocity, reaction target position as well as the effects of different degrees of spectral compression that have been used to extract the transition energies. Assuming that these states correspond to the same analogue structure (the presumed $[422]\frac{5}{2}^+$ ground-state band), MED can be extracted. The latter is also listed in Table 1 and plotted in Fig. 4(a). An important point to note is that although there is a slight downward shift in the energy of the $(\frac{7}{2}^+)$ state in ^{79}Y in the present work compared to the literature value, a similar effect is expected in the mirror nucleus, as a consequence of the previously discussed lifetime effects and isospin symmetry arguments. Hence we have assumed that these effects cancel out when extracting the MED for the $\frac{7}{2}^+$ states involved. The systematic uncertainty in the MED from this assumption is at the level of only ∼1 keV and is not considered significant.

Table 1
Measured γ-ray energies (in keV) and relative intensities (R.I.) of decays in the ^{79}Zr and ^{79}Y mirror pair. For ^{79}Y the measured γ-ray energies are compared with literature (Lit.) values, Ref. [22]. The recoil velocities ($\beta = \frac{v}{c}$) used in the Doppler-correction process to extract the energies are also detailed. The level energies (E_{J_i}) with errors and the calculated excitation energies from the NCCI calculations with charge-symmetry breaking terms included (E_{th}) are presented in keV for each nucleus. The final column contains the deduced MED values and their associated errors in keV.

$J_i \to J_f$	^{79}Zr					^{79}Y						MED$_{J_i}$
	E_γ	β	R.I.	E_{J_i}	E_{th}	E_γ	Lit.	β	R.I.	E_{J_i}	E_{th}	
$(\frac{7}{2}^+) \to (\frac{5}{2}^+)$	184(1)	0.298	100	184(1)	228	183(1)	184.0(5)	0.294	100	183(1)	226	1(1)
$(\frac{9}{2}^+) \to (\frac{7}{2}^+)$	230(2)	0.304	23(11)	416(2)	522	227(1)	227.0(5)	0.296	37(1)	411(1)	515	5(2)
$(\frac{9}{2}^+) \to (\frac{5}{2}^+)$	416(2)	0.304	18(11)	416(2)	522	411(1)	411.3(5)	0.296	17(2)	411(1)	515	
$(\frac{11}{2}^+) \to (\frac{9}{2}^+)$						316(1)	316.1(5)	0.304	17(2)†	726(1)	875	
$(\frac{13}{2}^+) \to (\frac{11}{2}^+)$						315(1)*	315.0(5)			1042(1)	1291	
$(\frac{11}{2}^+) \to (\frac{7}{2}^+)$	531(4)	0.304	21(13)	715(4)	886	543(1)	543.1(5)	0.304	13(2)	726(1)	875	−11(4)
$(\frac{13}{2}^+) \to (\frac{9}{2}^+)$						631(1)	631.1(5)	0.304	10(2)	1042(1)	1291	

* Assumed to be present following observation of 631-keV decay [22]. † Combined intensity of 315 and 316-keV decays.

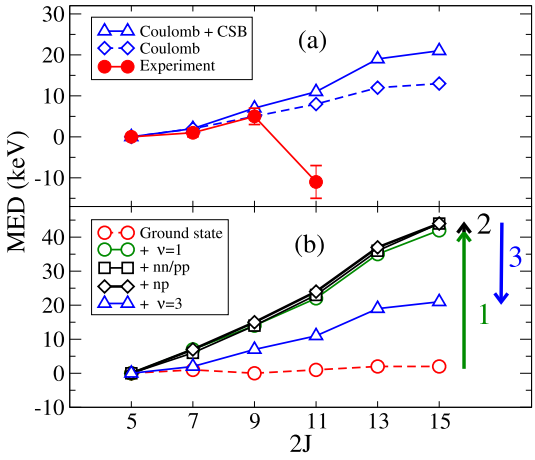

Fig. 4. (a) Mirror energy differences as a function of spin J for the tentatively assigned ground-state configuration of $[422]\frac{5}{2}^+$ in the ^{79}Zr/^{79}Y mirror pair. The calculations are shown with Coulomb only and Coulomb plus charge symmetry-breaking (CSB) terms included. (b) Calculations as a function of spin demonstrating how the various terms shown in the legend contribute to the final result that is represented by the blue triangles. The labels 1,2 and 3 refer to the groups of terms defined in Fig. 5 and the text. Note the blue triangles in (a) and (b) show the same final result.

Group		1			2					3	
Config.	g.s.	ν=1			nn/pp			np		ν=3	
total Ω	+5/2	+3/2	+1/2	+7/2	+5/2	+5/2	+5/2	+5/2	+5/2	+3/2	+7/2
N,Z or Z,N	39 40	39 40	39 40	39 40	39 40	39 40	39 40	39 40	39 40	39 40	39 40
[413]7/2				↑	●			↑↓		↓	↑
[301]3/2						●	●		↑↓		
[422]5/2	↑●	●●	●●	●	↑●	↑●	↑●	●	↑↓●	↑↓	↑↓
[303]7/2	●●	●●	●●	●●	●●	●	●	●●	↓●	●●	●●
[431]3/2	●●	↑●	●●	●●	●●	●●	●●	●●	●●	●●	●●
[440]1/2	●●	●●	↑●	●●	●●	●●	●●	●●	●●	●●	●●

Fig. 5. Configurations used in the NCCI calculations to obtain the results shown in Fig. 4. Full dots denote deformed $[N n_z \Lambda]K$ orbitals occupied by pairs of nucleons in the 39 or 40 subsystems. Empty dots with up (down) arrows denote orbitals occupied by single nucleons with individual positive, $\Omega = +K$ (negative, $\Omega = -K$) projections of angular momentum on the axial-symmetry axis.

4. Calculations

Compared with other odd-A nuclei previously studied, where variations of MED with J of 50-100 keV are common, the magnitudes of the MED extracted for the low-spin states of this mirror pair are unusually small – within ∼10 keV of zero – for the first few states. This may indicate that the rotational bands in these deformed systems are based on a highly stable configuration. Evidence for stable low-spin rotational structures have been observed in this mass region with fairly constant quadrupole moments being measured for the [422]5/2 structure in ^{83}Nb [24]. Furthermore, kinetic moments of inertia were found to be constant across several Nilsson configurations for both ^{79}Sr and ^{81}Zr prior to the first band crossing [25].

The shell-model approach to analysing MED used in other mass regions is not applicable here due to the large valence space required. Instead, we present here the results of a new approach to MED studies based on density-functional theory, and using the previously developed methodology of the no-core configuration-interaction (NCCI) model [15] which allows for full treatment of both rotational and isospin symmetries. The model includes isospin-breaking effects of both Coulomb and nuclear (charge-symmetry breaking, CSB) origin – the latter using next-to-leading order contact terms [26]. Using this method, the angular-momentum-projected states in ^{79}Zr and ^{79}Y were determined.

Calculations proceeded in two steps. First, standard single-reference Hartree-Fock (SRHF) [27] calculations were performed. For each calculation, the SRHF configurations were fixed by selecting 39 or 40 occupied single-particle deformed orbitals among the lowest ones appearing at large deformations in the Zr region. Configurations in mirror partners were always selected symmetrically, that is, those chosen for neutrons and protons in ^{79}Zr were, respectively, selected for protons and neutrons in ^{79}Y. Each selected configuration was converged separately, so its deformation and Coulomb/CSB polarisation effects were self-consistently determined. In each of the mirror partners, we established 40 low-lying SRHF configurations

In the second step, in both mirror partners we performed multi-reference Hartree-Fock (MRHF) NCCI calculations. These involved determining Hamiltonian and overlap matrix elements between all selected configurations and diagonalising the Hamiltonian matrix in a non-orthogonal basis. At this step, it was essential to use the Skyrme force SV$_{SO}$ [28], which, because of its density-independence, does correspond to a Hamiltonian. We stress that also in this step, the Coulomb/CSB terms were included in the Hamiltonian matrix elements. Calculations were performed using a new version of the HFODD solver [29], which was equipped with the NCCI module [15].

Analysis of the mixing properties of all 40 SRHF configurations revealed that only 10 of them have meaningful non-zero mixing coefficients with the ground-state configuration. The final calculations were therefore restricted to these 10 configurations. The resulting MED are shown in Fig. 4(a) and compared with the experimental data. Calculations with, and without CSB effects are shown, and it is clear that both Coulomb and CSB effects are relevant in this model.

The structure of the 10 configurations that mix with the ground state is shown in Fig. 5, and we have grouped the excited configurations, from left to right in Fig. 5 as (1) seniority $\nu = 1$ (denoting numbers of nucleons in broken pairs), (2) nn and pp (like-particle) and np (neutron-proton) pair excitations, and (3) $\nu = 3$ excitations. In Fig. 4(b) these groups are added (on top of the g.s. configuration) sequentially into the calculation, first group (1) (green arrow), then group (2) (black arrow) and finally group (3) (blue arrow). Calculations with and without the CSB effects are shown in Fig. 4. As one can see, the $\nu = 1$ ($\nu = 3$) configurations push MED towards positive (negative) values, with the net result being a smaller positive shift, whereas the pair configurations have negligible effect. Although it is clear that both Coulomb and CSB effects make contributions to the theoretical prediction, the data do not discriminate between calculations with and without CSB effects.

The comparison between the experiment and the model in Fig. 4(a) shows that the agreement is good for the first two excited states, followed by a discrepancy of around 20 keV for the tentatively assigned $\frac{11}{2}^+$ state. It should be noted in making this comparison that the predicted and experimental MED are both numerically small, compared with the results from systematic studies in lighter nuclei (e.g. Ref. [6]). Hence, although numerical discrepancies of the order of 20 keV may not normally be considered significant when comparing experimental MED with a model (e.g. shell-model approaches [6]), it is nevertheless clear that the model used in the present work does not account for the sudden change in the trend of the data for the $\frac{11}{2}^+$ state. We have not identified any explanation for this, and we have checked whether inclusion of the lowest $h_{\frac{11}{2}}\ [550]\frac{1}{2}$ deformed configuration may affect the MED of this state, but this configuration does not make any meaningful contribution to the states in the model. This is the first application of this new theoretical approach, and this work will be followed by a separate systematic study [30], where the model will be employed to investigate MED in lighter systems, where both experimental data and benchmark shell-model results exist.

5. Summary

In summary, a new tentative level scheme has been produced for the proton-rich system ^{79}Zr, allowing MED to be determined and analysed for the $A = 79$ mirror pair. This is the heaviest mirror pair for which excited states have been determined, and the first in the centre of the region of highly-deformed nuclei near $A \sim 80$. The experimental MED have been compared with the predictions of a new MED model rooted in density-functional theory that allows for the treatment and analysis of isospin-breaking phenomena. This new approach has the advantage of simultaneously taking into account strong non-perturbative quadrupole and isospin-breaking polarisation in a large configuration space, and at the same time, conserving symmetries of the system. Apart from comparing the new model to the frontier experimental data obtained in this work, a further study [30] will investigate application of this model to lighter systems, where benchmark shell-model results exist, and heavier systems, where obtaining guidance for future experimentation is essential.

This work was carried out at the National Superconducting Cyclotron Laboratory facility at MSU. The work was supported in part by STFC Grant numbers ST/M006433/1, ST/L005727/1, ST/P003885/1, The National Science Foundation (NSF) under Grant No. PHY-1565546, the Department of Energy (DOE) under Grant No. DE-SC0020451, the DOE National Nuclear Security Administration through the Nuclear Science and Security Consortium under Award No. DE-NA0003180 and the Polish National Science Centre under Contract No. 2018/31/B/ST2/02220. GRETINA was funded by the DOE Office of Science. Operation of the array at NSCL was supported by DOE under Grant No. DE-SC0014537 (NSCL) and No. DE-AC02-05CH11231 (LBNL). We acknowledge the CSC-IT Center for Science Ltd., Finland, for the allocation of computational resources.

Declaration of competing interest

The authors declare that they have no known competing financial interests or personal relationships that could have appeared to influence the work reported in this paper.

References

[1] R. Machleidt, I. Slaus, The nucleon-nucleon interaction, J. Phys. G, Nucl. Part. Phys. 27 (5) (2001) R69–R108, https://doi.org/10.1088/0954-3899/27/5/201.
[2] E. Wigner, On the consequences of the symmetry of the nuclear Hamiltonian on the spectroscopy of nuclei, Phys. Rev. 51 (1937) 106–119, https://doi.org/10.1103/PhysRev.51.106.
[3] A.P. Zuker, S.M. Lenzi, G. Martínez-Pinedo, A. Poves, Isobaric multiplet yrast energies and isospin nonconserving forces, Phys. Rev. Lett. 89 (2002) 142502, https://doi.org/10.1103/PhysRevLett.89.142502.
[4] M. Bentley, S. Lenzi, Coulomb energy differences between high-spin states in isobaric multiplets, Prog. Part. Nucl. Phys. 59 (2) (2007) 497–561, https://doi.org/10.1016/j.ppnp.2006.10.001, http://www.sciencedirect.com/science/article/pii/S0146641006000743.
[5] P.J. Davies, M.A. Bentley, T.W. Henry, E.C. Simpson, A. Gade, S.M. Lenzi, et al., Mirror energy differences at large isospin studied through direct two-nucleon knockout, Phys. Rev. Lett. 111 (2013) 072501, https://doi.org/10.1103/PhysRevLett.111.072501.
[6] M.A. Bentley, S.M. Lenzi, S.A. Simpson, C.A. Diget, Isospin-breaking interactions studied through mirror energy differences, Phys. Rev. C 92 (2015) 024310, https://doi.org/10.1103/PhysRevC.92.024310.
[7] A. Boso, S.M. Lenzi, F. Recchia, J. Bonnard, A.P. Zuker, S. Aydin, et al., Neutron skin effects in mirror energy differences: the case of ^{23}Mg—^{23}Na, Phys. Rev. Lett. 121 (2018) 032502, https://doi.org/10.1103/PhysRevLett.121.032502.
[8] D.M. Debenham, M.A. Bentley, P.J. Davies, T. Haylett, D.G. Jenkins, P. Joshi, et al., Spectroscopy of ^{70}Kr and isospin symmetry in the $T = 1$ fpg shell nuclei, Phys. Rev. C 94 (2016) 054311, https://doi.org/10.1103/PhysRevC.94.054311.
[9] J. Henderson, D.G. Jenkins, K. Kaneko, P. Ruotsalainen, P. Sarriguren, K. Auranen, et al., Spectroscopy on the proton drip-line: probing the structure dependence of isospin nonconserving interactions, Phys. Rev. C 90 (2014) 051303, https://doi.org/10.1103/PhysRevC.90.051303.
[10] K. Kaneko, S. Tazaki, T. Mizusaki, Y. Sun, M. Hasegawa, G. de Angelis, Isospin symmetry breaking at high spins in the mirror pair ^{67}Se and ^{67}As, Phys. Rev. C 82 (2010) 061301, https://doi.org/10.1103/PhysRevC.82.061301.
[11] R. Orlandi, G. de Angelis, P.G. Bizzeti, S. Lunardi, A. Gadea, A.M. Bizzeti-Sona, et al., Coherent contributions to isospin mixing in the mirror pair ^{67}As and ^{67}Se, Phys. Rev. Lett. 103 (2009) 052501, https://doi.org/10.1103/PhysRevLett.103.052501.
[12] K. Kaneko, Y. Sun, T. Mizusaki, S. Tazaki, Isospin nonconserving interaction in the $t = 1$ analogue states of the mass-70 region, Phys. Rev. C 89 (2014) 031302, https://doi.org/10.1103/PhysRevC.89.031302.
[13] K. Kaneko, Y. Sun, T. Mizusaki, S. Tazaki, Variation in displacement energies due to isospin-nonconserving forces, Phys. Rev. Lett. 110 (2013) 172505, https://doi.org/10.1103/PhysRevLett.110.172505.
[14] A.P. Zuker, A. Poves, F. Nowacki, S.M. Lenzi, Phys. Rev. C 92 (2015) 024320, https://doi.org/10.1103/PhysRevC.92.024320.
[15] W. Satuła, P. Bączyk, J. Dobaczewski, M. Konieczka, No-core configuration-interaction model for the isospin- and angular-momentum-projected states, Phys. Rev. C 94 (2016) 024306, https://doi.org/10.1103/PhysRevC.94.024306.
[16] X. Wu, H. Blosser, D. Johnson, F. Marti, R.C. York, in: Proceedings of the 1999 Particle Accelerator Conference (Cat. No. 99CH36366), vol. 2, 1999, pp. 1318–1320.
[17] D.J. Morrissey, B.M. Sherrill, M. Steiner, A. Stolz, I. Wiedenhoever, Commissioning the A1900 projectile fragment separator, Nucl. Instrum. Methods Phys. Res., Sect. B 204 (2003) 90–96, https://doi.org/10.1016/S0168-583X(02)01895-5, http://www.sciencedirect.com/science/article/pii/S0168583X02018955.
[18] D. Weisshaar, D. Bazin, P. Bender, C. Campbell, F. Recchia, V. Bader, et al., The performance of the γ-ray tracking array gretina for γ-ray spectroscopy with fast beams of rare isotopes, Nucl. Instrum. Methods Phys. Res., Sect. A 847 (2017) 187–198, https://doi.org/10.1016/j.nima.2016.12.001, https://www.sciencedirect.com/science/article/pii/S0168900216312402.
[19] S. Paschalis, I. Lee, A. Macchiavelli, C. Campbell, M. Cromaz, S. Gros, et al., Nucl. Instrum. Methods Phys. Res., Sect. A 709 (2013) 44–55, https://doi.org/10.1016/j.nima.2013.01.009.
[20] D. Bazin, J. Caggiano, B. Sherrill, J. Yurkon, A. Zeller, The S800 spectrograph, Nucl. Instrum. Methods Phys. Res., Sect. B 204 (2003) 629–633, https://doi.org/10.1016/S0168-583X(02)02142-0, http://www.sciencedirect.com/science/article/pii/S0168583X02021420.

[21] R.D.O. Llewellyn, M.A. Bentley, R. Wadsworth, H. Iwasaki, J. Dobaczewski, G. de Angelis, et al., Establishing the maximum collectivity in highly deformed $N = Z$ nuclei, Phys. Rev. Lett. 124 (2020) 152501, https://doi.org/10.1103/PhysRevLett.124.152501.

[22] M.J. Leddy, J.L. Durell, S.J. Freeman, B.J. Varley, R.A. Bark, C.D. O'Leary, et al., In-beam spectroscopy of ^{79}Y, Phys. Rev. C 58 (1998) 1438–1443, https://doi.org/10.1103/PhysRevC.58.1438.

[23] A. Lemasson, H. Iwasaki, C. Morse, D. Bazin, T. Baugher, J.S. Berryman, et al., Observation of mutually enhanced collectivity in self-conjugate $^{76}_{38}Sr_{38}$, Phys. Rev. C 85 (2012) 041303, https://doi.org/10.1103/PhysRevC.85.041303.

[24] N. Mărginean, D. Bucurescu, C. Rossi Alvarez, C.A. Ur, Y. Sun, D. Bazzacco, et al., High-spin behavior of multiple bands in the $n = z + 1$ nucleus ^{81}Zr: a possible probe of enhanced neutron-proton correlations, Phys. Rev. C 69 (2004) 054301, https://doi.org/10.1103/PhysRevC.69.054301.

[25] S.M. Fischer, C.J. Lister, M.P. Carpenter, N.J. Hammond, R.V.F. Janssens, E.F. Moore, et al., Mapping the periphery of deformation in the $a \sim 80$ region: a study of ^{83}Nb, Phys. Rev. C 75 (2007) 064310, https://doi.org/10.1103/PhysRevC.75.064310.

[26] P. Bączyk, W. Satuła, J. Dobaczewski, M. Konieczka, Isobaric multiplet mass equation within nuclear density functional theory, J. Phys. G, Nucl. Part. Phys. 46 (3) (2019) 03, https://doi.org/10.1088/1361-6471/aaffe4.

[27] N. Schunck (Ed.), Energy Density Functional Methods for Atomic Nuclei, IOP Publishing, 2019, pp. 2053–2563.

[28] M. Konieczka, P. Bączyk, W. Satuła, β-decay study within multireference density functional theory and beyond, Phys. Rev. C 93 (2016) 042501, https://doi.org/10.1103/PhysRevC.93.042501.

[29] N. Schunck, J. Dobaczewski, W. Satuła, P. Bączyk, J. Dudek, Y. Gao, et al., Solution of the Skyrme-Hartree-Fock-Bogolyubov equations in the Cartesian deformed harmonic-oscillator basis. (VIII) hfodd (v2.73y): a new version of the program, Comput. Phys. Commun. 216 (2017) 145–174, https://doi.org/10.1016/j.cpc.2017.03.007, http://www.sciencedirect.com/science/article/pii/S0010465517300942.

[30] P. Bączyk, W. Satuła, https://arxiv.org/abs/2010.06204, 2020.